

Analysis of the Genetic Model of the Extremely Narrow Channel Shallow Water Delta in DL-A Oilfield, Bohai Bay Basin

Hongjun Fan, Xingxing Kong,* Pengfei Mu, Dianshi Xiao, Dalin Zhao, Meijia Liu, and Mingwei He



Cite This: *ACS Omega* 2023, 8, 43978–43992



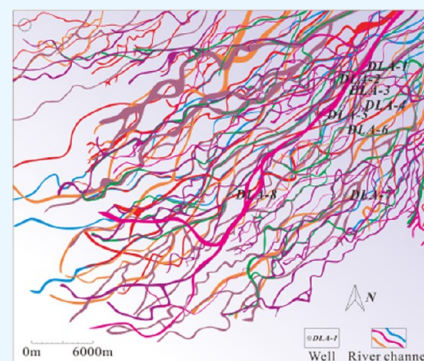
Read Online

ACCESS |

Metrics & More

Article Recommendations

ABSTRACT: In recent years, the oil and gas reserves discovered in shallow water deltas in China have continued to grow. The research on shallow water delta deposition models and depositional genesis is becoming more and more mature. In this latest discovery, a unique type of extremely narrow channel shallow water delta deposit was found at the top of the V oil group in the lower part of the Minghuazhen Formation during the Neogene period at DL-A Oilfield, located in the Bohai Bay Basin. The width of most single channels in this deposit measures between 100 and 200m, which is relatively rare and differs from existing research. To better understand this unique narrow channel shallow water delta deposit, a range of analysis methods were conducted including trace element analysis, major element analysis, grain size analysis, core observation, casting thin section observation, 3D seismic analysis, and other methods. These analyses were used to determine the sedimentary environment and sedimentary genesis of the deposit in the study area. The results show the following: (1) The top of the V oil group in the lower part of Minghuazhen Formation was deposited with a strong oxidizing environment. In the early stage, the climate was dry and cold, and gradually changed to warm and humid in the late stage. (2) Due to the frequent exposure to the surface, obvious weathered surfaces and sedimentary discontinuities were observed on the cores; the particle size analysis shows that the lamina types developed in the study area are clastic–clay laminae and clay–clastic laminae, which are mostly developed in shallow lakes area. (3) Observations of cores and thin sections also indicated that the hydrodynamic conditions frequently changed in the study area, alternating between strong and weak hydrodynamic conditions in a short period due to the alternating occurrence of flood and dry periods during the rainy season. Weak hydrodynamic conditions and slow water flow result in insufficient undercutting and sidecutting of rivers. The alternating occurrence of flood periods and dry periods has led to the development of crevasse splays and frequent river channel diversions, resulting in the inability of long-term stable development of the river channel. Besides, the change of water level has also led to the rebuilding of the river. Therefore, the multiple effects led to the formation of an extremely narrow channel shallow water delta. The accuracy of the sedimentary model is verified by a comparative study of the Shaliu River and Buha River in the modern Qinghai Lake. The new extremely narrow channels deposition model proposed this time further improves the deposition theory. At the same time, the modern depositional characteristics of the Shaliu River and Buha River also reveal the reservoir deposition between channels that cannot be distinguished by seismic data, providing guidance for the development of oil and gas in the study area.



INTRODUCTION

In recent years, with the continuous development of oil and gas exploration and development in China's continental basins, shallow water delta oil and gas reservoirs have been discovered in the Songliao Basin, Ordos Basin, and Bohai Bay Basin. Among them, river-controlled shallow water deltas dominated by rivers account for a large proportion.^{1–6} Obviously, large shallow water delta reservoirs in the depression lake basin have made important contributions to the growth of China's oil and gas reserves.^{7,8} The remarkable achievements in oil and gas exploration in shallow water delta reservoirs have attracted wide attention from geologists, and a large number of studies have been carried out on the genesis and depositional patterns of shallow water deltas.^{9–11}

The earliest research on deltas can be traced back to Gilbert of the US Geological Survey, who conducted research on the Pleistocene Lake Bonneville Delta during the period from 1885 to 1890.^{12,13} And Fisk (1954) proposed the concept of shallow water delta when studying the Mississippi Delta.¹⁴ Then, a lot of researchers found that water depth is an important controlling factor for the development of shallow water deltas.^{13,15,16}

Received: August 16, 2023
Revised: October 16, 2023
Accepted: October 19, 2023
Published: November 6, 2023



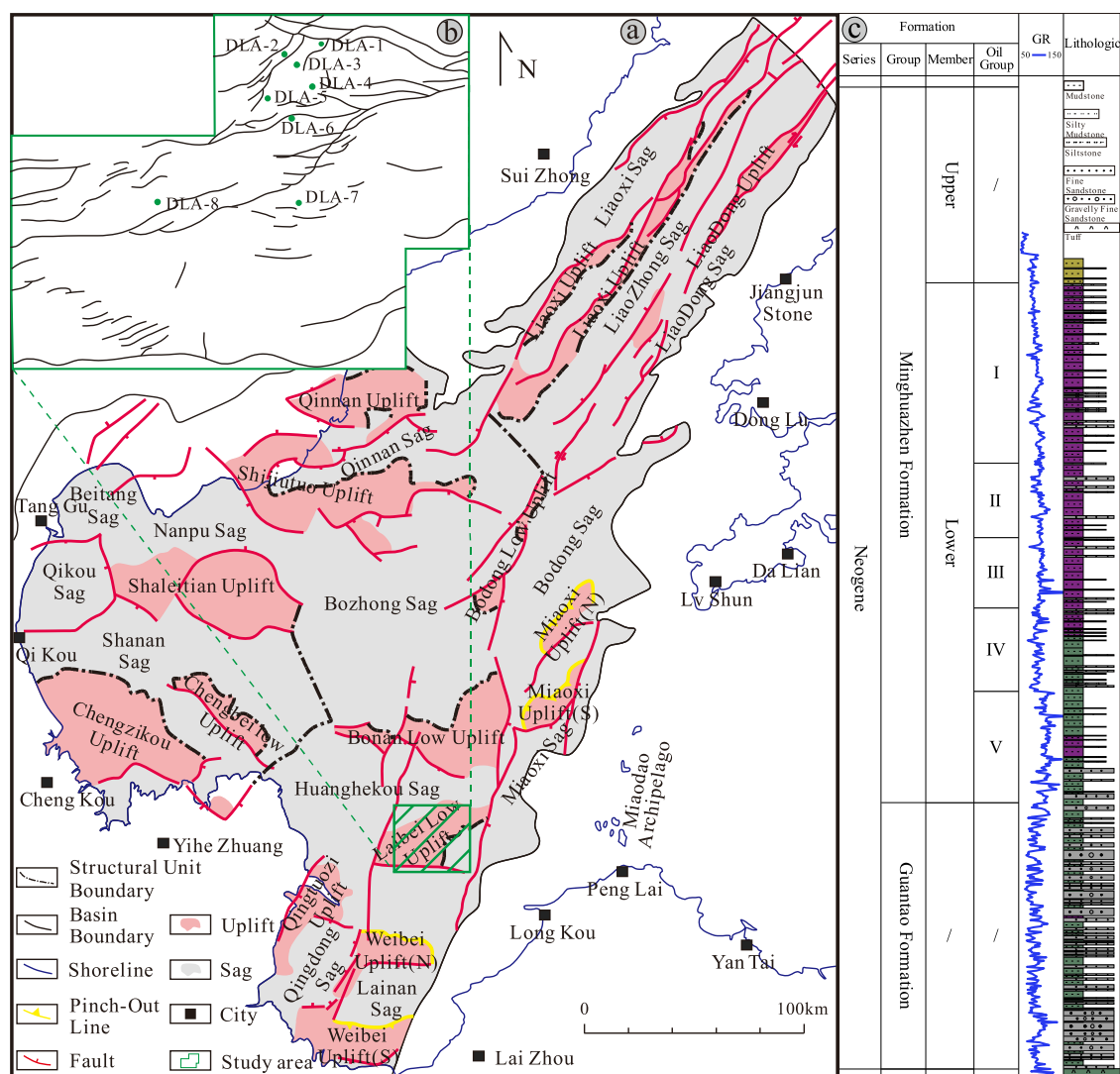


Figure 1. Location of the study area ((a) structure map of Huanghekou Sag, Bohai Bay Basin; (b) constructional location map of DL-A oil field; (c) the comprehensive stratigraphic column of the study area).

Existing studies have shown that shallow water deltas have the following characteristics: the delta front is open, the sedimentary water is shallow, and it is often exposed to the surface.^{8,17}

According to Zhang et al.'s sedimentary research on modern Dongting Lake and Poyang Lake, shallow water deltas are divided into branch-shaped distributary channel deltas dominated by river and continuous distributary sand dam deltas dominated by lake current.¹¹ Xuanjun et al. studied the Baoqian delta of the Upper Cretaceous in southern Songliao Basin and the modern Ganjiang delta in Poyang Lake and found that there are mainly two types of shallow water deltas developed: deep water deltas are generally lobe-shaped; shallow water deltas are generally bird-foot-shaped, with no obvious differentiation of sedimentary subfacies. And sedimentary microfacies are dominated by distributary channels and interdistributary bays.¹⁸

Zhu et al. through the study of the shallow water delta of the Qingshankou Formation in the Qijia area of the Songliao Basin showed that the extension of the distributary channels in the shallow water delta is related to the depth of the lake. When the lake water is shallow, the extension length of the river channels exceeds 50 km, and when the lake water is deep, the extension distance of the channels does not exceed 30 km.⁹ Through the

simulation of the development and evolution of the shallow water deltas, Huang et al. found that the frequency of lake level oscillations appears to be a significant controlling factor in determining the deltaic architecture within the deltaic systems.¹⁹ Lou et al.'s research has also shown that the frequent fluctuations of the lake level will reshape the deposition of shallow water deltas and make the sand bodies sheet-like.^{8,17}

Except water depth, climate also affects the deposition of shallow deltas. Zhu et al.'s study on the Cretaceous Quantou Formation in Sanzhao Sag, Songliao Basin shallow water deltas showed that climate is the main controlling factor for the spread of shallow water deltas. When it was dry, the lake basin shrinks, and the extension distance of the distributary channels generally exceeds 20 km, and the width is 800–1800 m. When it was humid, the lake expanded, the river branched off frequently, and formed reticular distributary channels that were narrow and deep, and the length of the channels was less than 15 km and the width was 500 to 1600 m³. A large number of studies on China's shallow water deltas indicate that the development of shallow water deltas should meet the following conditions: large lake basin with gentle slope, dry and hot paleoclimate, frequently

Table 1. Basic Information of the Samples

well name	depth/m	lithology	formation	number of samples			
				trace element	major element	particle size	
DLA-1	1425–1595	shale	Neogene Minghuazhen Formation	7			
DLA-3	1425–1605	shale		9			
DLA-5	1439–1444	sandstone					4
	1445–1605	shale		6			
	1000–1605	shale				21	
DLA-6	1467–1478	sandstone					4
	1400–1555	shale		7			
DLA-8	1485–1630	shale		4			

fluctuating lacustrine level, turbulent extremely shallow water, and sufficient sediment supply.^{3,20–22}

In the existing studies, the sedimentary characteristics of shallow water deltas are obvious, and the single channel width is large, generally greater than 500 m.^{3,9–11,19} However, a new type of shallow water delta deposition was discovered in the DL-A oilfield in the Bohai Bay Basin. Seismic geobody interpretation and stratal slices showed that the channels in the study area had obvious depositional features, and the width of the river channels is generally less than 200 m, the river curvature is low, the development of other microfacies cannot be observed on the stratal slices, and the branch channel is not developed. The shallow water delta deposition model described here differs significantly from existing delta deposition models, making it challenging to study reservoir and sand body distribution characteristics. The lack of geological knowledge further increases development risks, as there are no existing sedimentary models to reference. Therefore, this study focuses on the extremely narrow channel shallow water delta deposits in the upper Minghuazhen Formation of the Neogene in the DL-A Oilfield in the Bohai Bay Basin. By utilizing trace element analysis, major element analysis, core observation, casting thin section, grain size analysis experiments, 3D seismic data, and other methods, in conjunction with modern sedimentary comparisons, a genetic model was analyzed and a new shallow delta sedimentary model was proposed. By employing this model as a guide, the dominant reservoir area can be predicted, and the development of the oil field can be effectively guided to reduce development risks.

■ GEOLOGICAL BACKGROUND

DL-A Oilfield is located in the northeastern part of the Laibei Low Uplift in the Bohai Bay Basin, with the Huanghekou Sag in the north and Laizhou Bay Sag in the south (Figure 1). The north and south sides of the Laibei Low Uplift are divided by extensional faults, and the east and west sides are controlled by the Tanlu strike-slip fault. The extensional stress and the strike-slip shear stress jointly control the formation and evolution of the Laibei Low Uplift.²³ The Laibei area developed in sequence of the Pre-Cenozoic (Jurassic and Cretaceous), Paleogene Kongdian, Shahejie and Dongying formations, Neogene Guantao and Minghuazhen formations, and Quaternary Pingyuan formations. And there is an unconformity between the Paleogene and the Neogene.^{2,24,25} The Minghuazhen Formation is further divided into upper and lower parts (Figure 1c). Based on lithostratigraphy, climate cycles, and sequence subdivision, two third-order cycles are identified in the lower part of Minghuazhen Formation, corresponding to 2 third-order sequences and 5 fourth-order sequences. According to 5 fourth-order sequences, the lower part of Minghuazhen Formation is

divided into five oil groups from top to next: I, II, III, IV, and V (Figure 1c). The target layer of this study is the top of the V oil group.^{2,26,27}

Predecessors' studies on the Neogene deposits in the Bohai Bay indicate that the river and lake sediments around the Bohai Bay Basin developed well during the Miocene.^{1,23,28,29} In addition, the Neogene was the period of contraction during the formation of the Bohai Bay Basin, with the characteristics of stable structure, slow deposition rate, and flat terrain. The characteristics of paleontological assemblage, geophysics, lithofacies and facies sequence assemblage, and sandstone percentage all show that the lake water body was relatively shallow during the Neogene deposition period, and a large area of shallow water delta sedimentary system was formed.^{1,21,28} In this study area, the lake water during the deposition of the Upper Neogene in the Laibei Low Uplift was also relatively shallow, and the shallow water delta deposition was the main deposition system.^{23,30,31}

■ SAMPLES AND METHODS

A total of 62 samples were collected this time, all from the Neogene Minghuazhen Formation. The lithology is mainly sandstone and shale. The trace element tests were carried out on 33 shale samples; major element tests were carried out on 21 shale samples; and particle size tests were carried out on 8 sandstone samples. The basic information on the samples is shown in Table 1.

Trace Element. This time, a total of 33 shale samples from 5 wells were measured for trace elements. The samples need to be crushed in an agate mortar to more than 200 mesh, they were then placed in a muffle furnace and heated at 500 °C for 2 h to eliminate the influence of organic matter in mudstone and crystal water in minerals, then it was dissolved with HF + HNO₃ solution and tested on inductively coupled plasma mass spectrometer (ICP-MS).

Major Element. A total of 21 shale samples from Well DLA-5 were tested for major elements. The samples were crushed to more than 200 mesh and then heated to 950 °C in an open muffle furnace; then, they were dissolved in a mixture of HClO₄ and HF. The testing was performed on an Axios-mAX wavelength-dispersive X-ray fluorescence spectrometer.

Particle Size. A total of 8 sandstone samples from 2 wells were analyzed for particle size. The particle size analysis adopts a combination of sieving method and laser particle size method, and the detection method refers to SY/5434–2009 “Clastic Rock Grain Size Analysis Method”. The measuring instrument is the Mastersizer-2000 laser particle size analyzer produced by Malvern, England, with a measuring range of 0.02–2000.00 μm, combined with the sieving method, the maximum range is 3000.00 μm, and the repeat error is less than 1%.

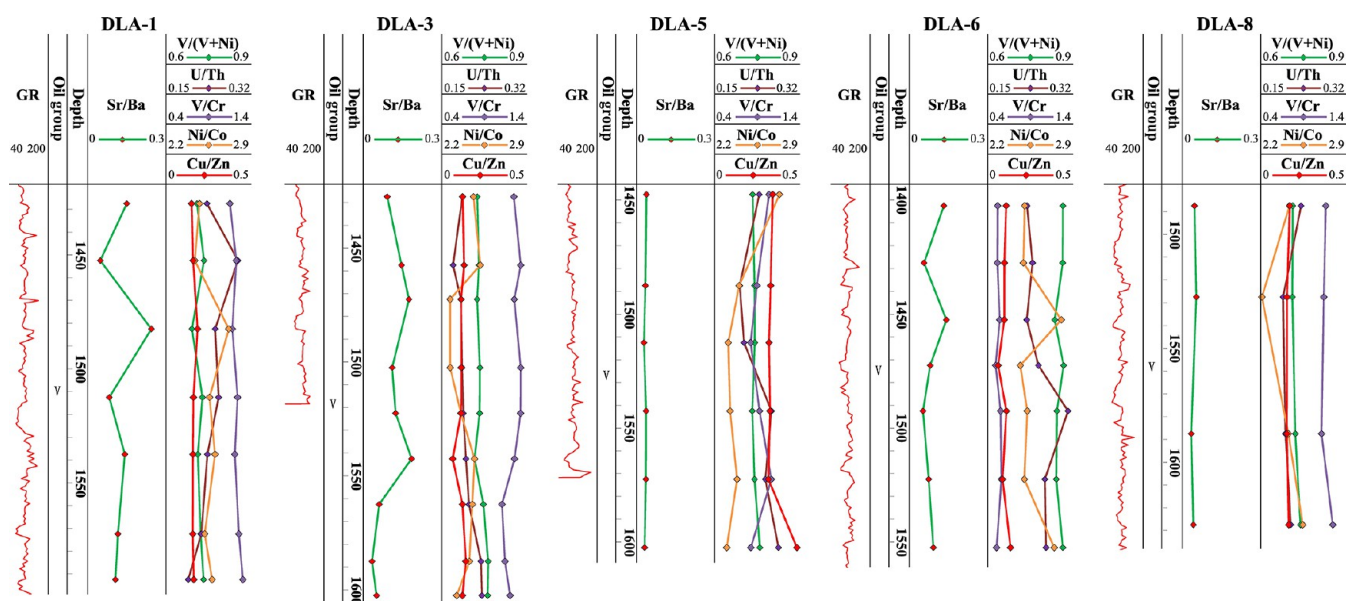


Figure 2. Distributions of paleo-salinity and paleo-redox proxies in the study area.

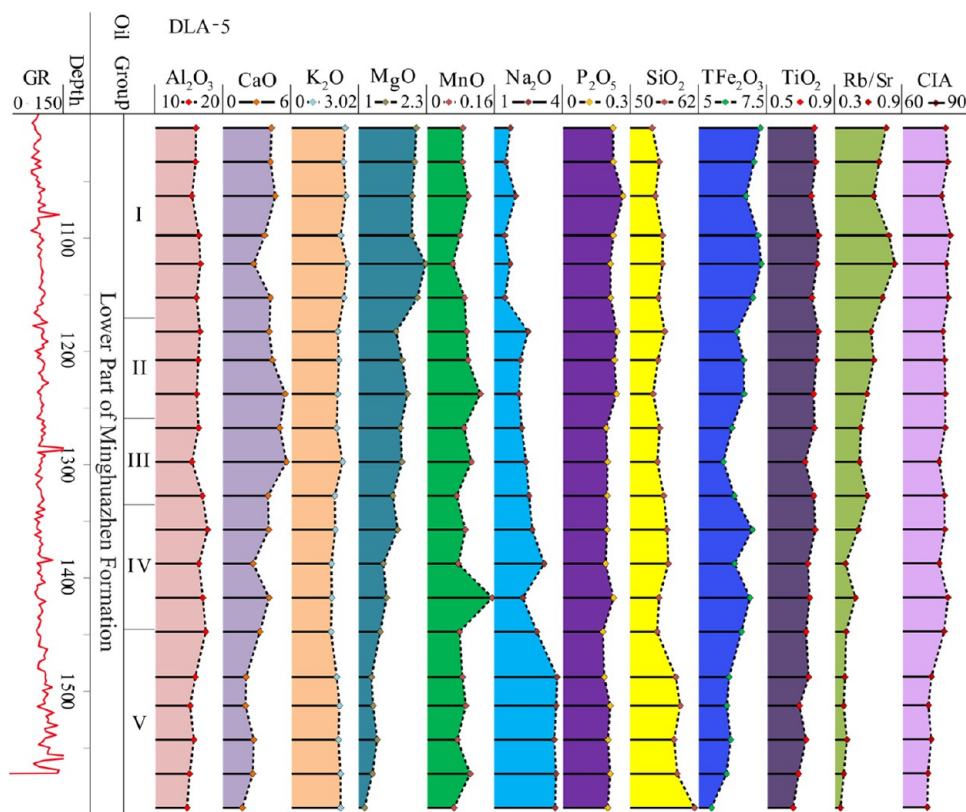


Figure 3. Variation characteristics of major elements, value of Rb/Sr, and the CIA value in the lower part of the Minghuazhen Formation in well DLA-5.

RESULT

Trace Element. The redox state of the sedimentary environment controls the enrichment of the redox-sensitive trace elements in sediments or sedimentary rocks.^{32–34} In addition, the paleo-salinity, paleo-climatic conditions, etc. of the sedimentary environment will also affect the enrichment of trace elements.^{35,36} By analyzing the ratio of different elements and other information, it can effectively reflect sedimentary

information such as paleo-salinity, paleo-redox conditions, and paleo-climate.^{36–38}

Paleo-Salinity. The ratio of Sr/Ba is one of the most commonly used methods to judge paleo-salinity.^{39,40} According to many studies, when Sr/Ba is greater than 1.0, it reflects the marine environment, and when it is less than 0.6, it is a freshwater environment; when the value is 0.6–1.0, it reflects the semisalinity water deposits in the transition zones between oceans and continents.^{41,42} The Sr/Ba values of the samples

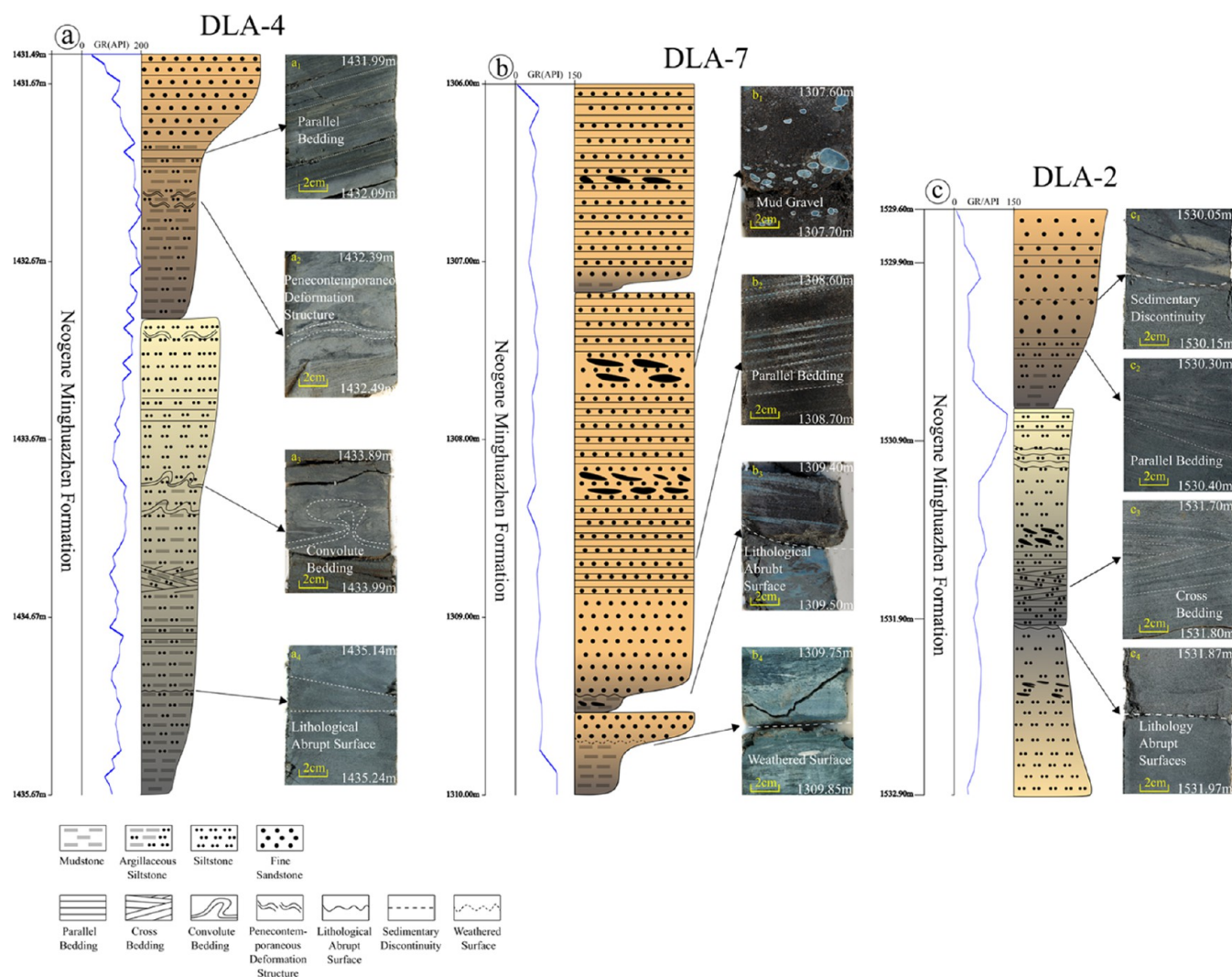


Figure 4. Core histograms of the three core wells ((a) Sedimentary structure characteristics of the core in well DLA-4: (a₁) parallel bedding, fine sandstone bands can be seen in siltstone; (a₂) penecontemporaneous deformation structure; (a₃) convolute bedding; (a₄) lithological abrupt surface. (b) Sedimentary structure characteristics of the core in well DLA-7: (b₁) sandstone with mud gravel; (b₂) parallel bedding; (b₃) lithological abrupt surface; (b₄) weathered surface. (c) Sedimentary structure characteristics of the core in well DLA-2: (c₁) sedimentary discontinuity; (c₂) parallel bedding; (c₃) small cross-bedding; (c₄) lithology abrupt surfaces).

from the V oil group this time are all less than 0.6, mainly distributed between 0.1 and 0.3, which is an obvious freshwater deposition environment (Figure 2).

Paleo-Redox Conditions. The geochemical behaviors of valence-variable elements V, U, etc. are closely related to the redox conditions of the sedimentation and diagenesis.^{43,44} In a dysoxic condition, V and U are low in price and easy to be enriched. Therefore, $V/(V + Ni)$, U/Th , and other parameters are usually used as geochemical parameters indicating the paleo-redox conditions.^{37,45} The analysis results show that the U/Th of the V oil group in the study area is mainly distributed between 0.2 and 0.3, and the $V/(V + Ni)$ value distribution around 0.7 reflects the obvious oxci condition (Figure 2). In addition, the ratios of V/Cr , Ni/Co , and Cu/Ni are often used to indicate the redox environment.^{46,47} The inconsistent results indicate that the element compositions have complex controlling factors and should be used with caution when reflecting redox conditions.⁴⁸ However, the accuracy of identification can be increased through comprehensive discrimination of multiple indicators.⁴⁹ The value of V/Cr in the study area is distributed between 0.19

and 133, with an average value of 1.02; the value of Ni/Co is distributed between 2.21 and 2.80, with an average value of 2.47; the value of Cu/Zn is distributed between 0.06 and 0.48, with an average value of 0.17. The distribution of the above three redox-sensitive trace element parameters also indicates an oxygen-enriched depositional environment. In addition, drilling data also show that the mudstone cuttings on the top of the V oil group are mostly purple-red (Figure 1c), further confirming the strong oxci condition in this area.

Major Element. The content, combination, and ratio of the various elements in the sediment are inextricably linked to the physical and chemical conditions in the sedimentary environment, which can reflect changes in the sedimentary environment and climate background. During the processes of leaching, migration, and accumulation of geochemical elements, the activities of K, Na, Ca, Mg, Si, Fe, and Al generally decrease in sequence.⁵⁰ Therefore, under humid conditions, K and Na are the first to be lost and enriched under dry conditions; Si, as the main rock-forming mineral, exists in the form of quartz and exhibits relatively stable chemical properties. Under warm and

humid climate conditions, it leaches before Al and Fe. Under dry and cold climate conditions, chemical weathering and leaching are weak, resulting in relatively enriched Si.^{51–53} Therefore, high values of K, Na, and Si indicate dry and cold climates with weak chemical weathering. The high values of Al and Fe reflect strong chemical weathering and warm and humid climate. Ca and Mg are most easily enriched under semiarid climate conditions. The enrichment of different elements can be observed to infer the paleo-climatic conditions.

Paleoclimate. The test results of the major elements in the lower part of Minghuazhen Formation in Well DLA-5 show a clear trend: the content of Na and Si is the most concentrated in the V oil group and gradually decreases upward, while the content of Al and Fe are the most concentrated at the top (Figure 3). The changing trends of the contents of various elements reveal the dry and cold climate characteristics of the V oil group in the lower part of Minghuazhen Formation (Figure 3). It also reveals that during the development of the lower section of the Minghuazhen Formation, the climate gradually changed from dry and cold to warm and humid.

Rb/Sr is usually used to indicate the degree of paleoweathering, and sometimes it is also used to study paleo-climatic characteristics.⁵⁴ In a lacustrine basin, when the climate is warm and humid, the Rb/Sr value increases,⁴⁷ but under relatively dry and cold conditions, the Rb/Sr value is relatively low.^{30,55} The average value of Rb/Sr of V oil group in the study area is 0.39, and the ratio gradually increases upward, which also reveals the relatively dry and cold climate characteristics during the development of V oil group in the study area, consistent with previous studies.³⁰

The chemical index of alteration (CIA) is also one of the more commonly used parameters indicating paleoclimate changes.^{56–58} The value of CIA is calculated by the following formula:

$$(Al_2O_3)/(Al_2O_3 + CaO^* + Na_2O + K_2O) \times 100$$

where CaO* refers to the CaO content in the silicate fraction.^{59,60} During chemical weathering, the Al³⁺ and Ti⁴⁺ tend to be concentrated, while Ca²⁺, K, and Na tend to leach.⁵⁷ Therefore, the level of CIA can be used to evaluate the chemical weathering process.^{61,62} High CIA values reflect strong chemical weathering in humid conditions, while low values indicate weak or no chemical weathering in arid or cold climates.⁶³ The CIA values in the study area are distributed between 71.47 and 81.76, with an average value of 77.64 and gradually increasing upward, which also reveals the paleoclimate of arid and cold in the early period and humid in the late period (Figure 3).

Cores. As the most direct evidence reflecting the underground sedimentary characteristics, cores cannot be ignored in the analysis of sedimentary environment.^{64,65} The sedimentary characteristics of core samples from the top of the V oil group were analyzed for three wells in the study area.

DLA-4. The location of the well DLA-4 is shown in Figure 1b. The core of Well DLA-4 is located at the top of the V oil group. The core exhibits a predominantly brown or light gray color, and the lithology is mainly composed of fine sandstone and siltstone (Figure 4a). The sedimentary stability is significantly poorer than that observed in Well DLA-2. The sedimentary structure exhibits rapid changes. The lowermost part shows a massive bedding. In the middle section, alternating occurrences of penecontemporaneous deformation structures, gravity gliding tectonics, and parallel bedding can be observed (Figure 4a₂,a₃), while continuous parallel bedding is present at the top (Figure

4a₁). In contrast to Well DLA-2, the core of Well DLA-4 exhibits more frequent changes in bedding and hydrodynamics. Coarse-grained deposits and fine-grained deposits often alternate frequently, forming rhythmic layers. Furthermore, numerous lithological abrupt surfaces are present (Figure 4a₄).

DLA-7. Well DLA-7 is located in the center of the study area (Figure 1b). The lithology observed in the core is mainly gray-brown fine sandstone (Figure 4b). At the bottom of the core, there is a 0.3 m green-gray mudstone layer, followed by a 0.15 m layer of gray-brown fine sandstone and a 0.1 m layer of gray mudstone. Moving upward, the upper part of the core consists of a 3.45 m long section of gray-brown fine sandstone intercalated with thin mudstone layers. The core exhibits a reverse granular order, with the grain size becoming coarser toward the top. At the bottom of the core, there are noticeable lithological abrupt surfaces and weathered surfaces (Figure 4b₃,b₄), indicating clear sedimentary discontinuities. Throughout the core, gray-green mud gravel can be observed within the gray-brown sandstone in various locations. The diameter of the mud gravel ranges from 0.1 to 5 cm, and the long axis of the gravel is consistently arranged parallel to the bedding planes (Figure 4b₁). In the upper portion of the core, the sedimentary structure is predominantly characterized by parallel bedding, with minimal overall variation. However, distinctive gray-green mudstone layers can be observed within the parallel bedding (Figure 4b₂).

DLA-2. Well DLA-2 is located in the northern part of the study area (Figure 1b). The core exhibits a predominantly brown or light gray color, and the lithology is mainly composed of fine sandstone (Figure 4c). The bottom of the core is fine sandstone of about 3 m, mudstone of about 0.1 m, and argillaceous siltstone of 0.15 m in the middle, and medium sandstone of about 1 m at the top. The grain size shows a reverse granular order, with coarser grains found toward the top. The sedimentary structure is relatively simple, dominated by parallel bedding (Figure 4c₂), occasionally small cross-bedding (Figure 4c₃), with small vertical changes. A sedimentary discontinuity surface is observed (Figure 4c₁), exhibiting abrupt changes in bedding direction and sedimentary lithology near the surface. Moreover, several abrupt sedimentary lithology surfaces are also present (Figure 4c₄).

Casting Thin Section. Observation of cast thin sections also reveals rapid changes in the particle size of the rock, and distinct rhythmic patterns can be observed on some cast thin sections (Figure 5). The upper portion of the V oil group is primarily composed of medium sandstone and fine sandstone, with occasional occurrences of sandy mudstone. In sandy mudstone, prominent quartz and feldspar grains can be observed, with the long axis of the grains exhibiting relative stability, and showing weak banding with the argillaceous matrix (Figure 5c,d). The alternation between dark argillaceous matrix and bright quartz is particularly evident in Figure 5. Under the microscope, the key features are clearly defined light and dark bands, presenting obvious rhythmic bedding. The bright bands consist predominantly of quartz and feldspar, characterized by a low clay content, large particle size, and high maturity, indicative of strong hydrodynamics (Figure 5).

Grain Size. The cumulative probability curve in the study area presents an obvious two-stage type, with obvious inflection points (Figure 7). The two-segment curves are suspension curves, and the two sides of the fine truncation point represent two transport modes.⁶⁶ Among the two segments, the curve on the left has a certain slope, corresponding to graded suspended particles. And the curve on the right corresponds to a uniform

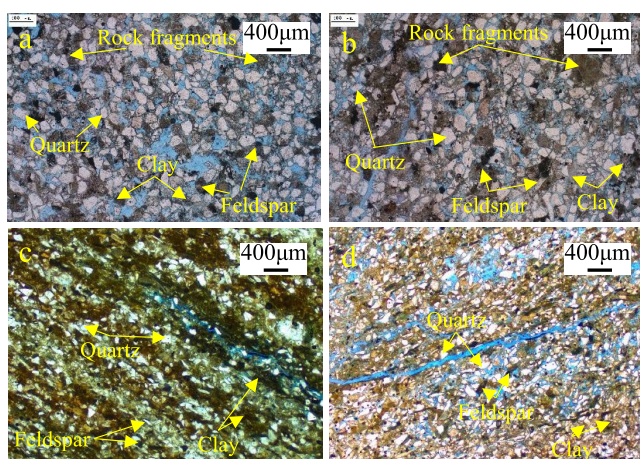


Figure 5. Casting thin sections of well DLA-4 ((a) 1424.00 m, fine- and medium-grained lithic feldspar sandstone; (b) 1429.00 m, medium-grained lithic feldspar sandstone; (c) 1433.99 m, sandy mud shale; (d) 1435.20 m, sandy mudstone).

suspension transport mode, which corresponds more to clay deposition (corresponding to the dark bands in Figure 6).

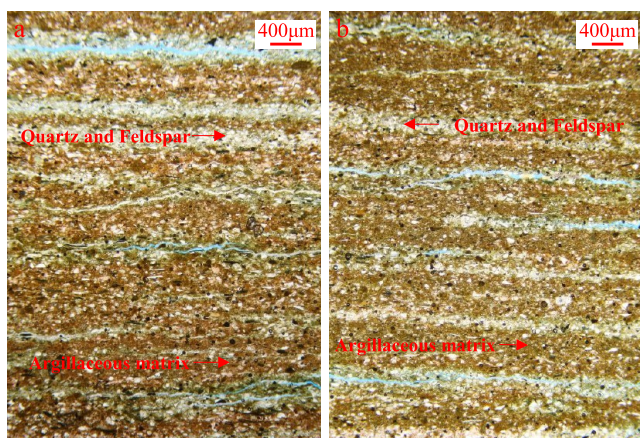


Figure 6. Rhythmic bedding observed in Well DLA-4 ((a) 1432.04 m, sand-bearing shale; (b) 1432.18 m, sand-bearing shale).

According to the classification of Tao et al., the lamina types developed in the study area are clastic–clay laminae and clay–clastic laminae, which are mostly developed in shallow lake areas.⁶⁶ The clastic and clay-clastic laminae of shallow lake sediments often form a complete combination of bright and dark laminae (Figure 6). This combination of light and dark laminae is formed by the alternation of seasons.^{66–69}

Seismic Sedimentology. Different from classic seismic stratigraphy, seismic sedimentology is a discipline that uses the relationship between seismic amplitude (attribute) with lithology and the relationship between spatial reflection mode with sediment morphology to study sedimentary lithology, physical properties, geomorphology, sedimentary structure, and sedimentary environment.^{70–72} Seismic geobody interpretation and stratal slicing are important techniques for studying seismic sedimentology. Stratal slicing can map seismic attributes of geological time surfaces.¹⁰ Compared to time slices and horizon slices, stratal slices are superior for use in faulted and wedged sequences.^{73–76} Seismic geobody interpretation can display the

distribution of sand bodies in a three-dimensional space and has a good effect on delta and river sediment system analysis.^{27,76,77}

This time, geobody interpretation and stratal slicing were carried out on the top of the V oil group in the study area. Through multiattribute optimization, the root-mean-square (RMS) amplitude attribute was selected to characterize the reservoir distribution in the study area. The effective frequency bandwidth of the seismic data used is about 8–55 Hz, and the main frequency is 35 Hz. Geobody interpretation and stratal slice show that the river sedimentary system in the study area is very well developed, the source direction is clear, and the characteristics of the river from the northeast to the southwest are obvious (Figure 8).

The river channels in the northwest direction of the study area exhibit distinct characteristics, including a meandering river shape and a single channel width generally exceeding 300 m (Figure 8). In the southeast of the study area, a different type of channel development is observed. Geobody interpretation indicates that the rivers in this area form multiple branches that gradually diverge as they approach the lake, with a single channel width of approximately 200 m. In the middle of the study area, there is a prevalence of extremely narrow channel sediments (Figure 8b). This type of sedimentary characteristic is relatively rare in existing studies. The development of river channels in this region displays the following traits: a narrow width for a single channel, usually less than 100 m, an extended length for the narrow channel, and a lack of developed sand bodies at the end of the river. Currently, there are limited studies investigating the genesis and depositional patterns of such extremely narrow channels. Accurately identifying the formation and sedimentation patterns of these channels has become a key issue that hinders oil and gas exploration and development in this area.

Further refinement of the stratal slices reveals the development process of the narrow river in the study area: the narrow and long channels run through the entire development process of the top V oil group, from bottom to top, the mainstream domain gradually transitions from northwest to southeast. The channel width is narrow in the early and late stages and wider in the middle stage (Figure 9). The multistage development of the river channels has led to the crossing of the river channels in the vertical and horizontal directions (Figure 8). During the development process, the length of the river in the study area tends to decrease, and the location where the branch begins gradually moves toward the provenance, indicating the expansion of the water body. This change is mainly due to the gradual transformation of the climate from dry and cold to warm and humid during the development of the lower part of the Minghuazhen Formation (Figure 3).

DISCUSSION

The trace elements show that the V oil group in the study area was deposited in a freshwater environment, and the values of V/(V + Ni) and U/Th indicate a strong oxidizing environment. The mudstone cuttings in the V oil group in the study area are mostly purple-red, which also confirms the strong oxidizing environment and also shows that the water body was shallow at that time. In addition, obvious evidence can be observed from the cores. Obvious sedimentary discontinuities and even weathered surfaces are observed on the cores of the three wells in the study area, indicating that the top of the V oil group in the study area is often exposed to the surface. Grain size changes in multiple scales and lithological abrupt surface were

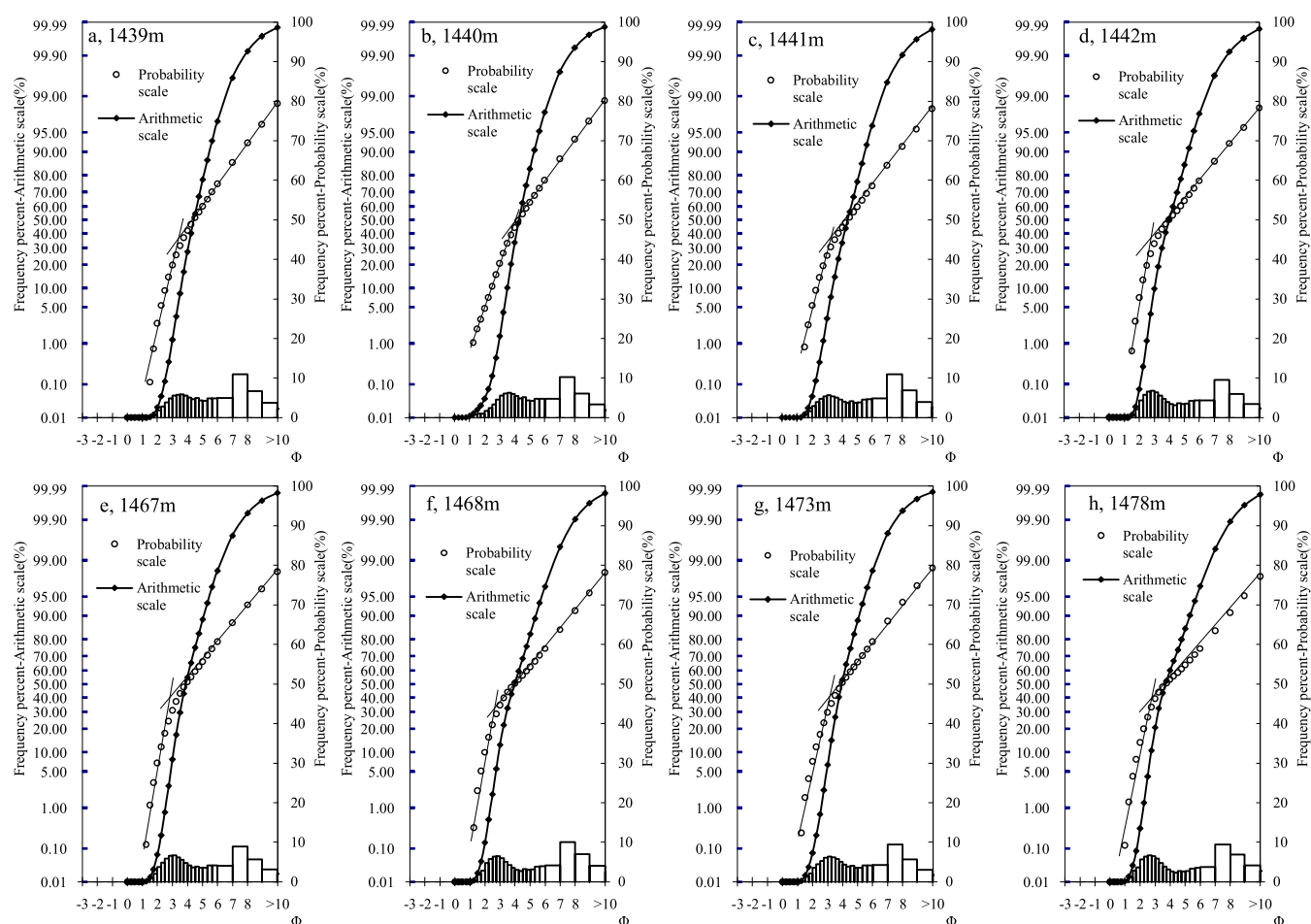


Figure 7. Characteristics of cumulative probability curve in the study area ((a–d) well DLA-3; (e–h) well DLA-5).

observed on the cores, and obvious rhythmic bedding was also observed on the cast thin section, indicating frequent changes in hydrodynamics. The changes of major elements and the ratio of Rb/Sr in the lower part of the Minghuazhen Formation show that the overall climate of the V oil group in the study area is dry and cold.

Therefore, the sedimentary environment of the study area has the following characteristics: overall weak hydrodynamic conditions, and the undercutting and sidecutting effects of rivers are weak. At the same time, the alternating occurrence of flood period and dry period during the rainy season in a short period of time resulted in frequent changes in hydrodynamic conditions and sediment grain size, and a large number of crevasse splays developed. Under the accumulation of multiple floods, when a large-scale flood period comes, the river channel is easily diverted at the location of the crevasse splay. The abandoned river channel is filled by the overflow deposits of the new channel, and it is weathered when exposed (Figure 4). The advent of short-term rain causes hydrodynamic changes in a small area, forming rhythmic bedding (Figure 6). At the same time, due to the shallow water body and frequent changes in flood period and dry period, the water level will fluctuate frequently, and the river will be reformed and diverted. Weak hydrodynamic conditions and frequent river diversions have led to the development of extremely narrow channels (Figure 10).

In order to verify the above inferences, modern sedimentary analysis found that the development of rivers on the periphery of Qinghai Lake is very similar to the study area. The climate type

of Qinghai Lake is plateau continental climate, with low temperature, large temperature difference between day and night, little and concentrated rainfall, severe cold and long winters, and cool and short summers. There are more than 50 rivers in the Qinghai Lake basin, among which the Buha River and the Shaliu River are more famous.

The sedimentary systems of the Shaliu River and the Buha River verified the depositional process of the above-mentioned narrow channels. Shaliu River is located in the northern of Qinghai Lake, China, with a total length of 106 km and a drainage area of 1442 km². The upper reaches of the river are a complex form of meandering and braided rivers. Buha River is located in the west of Qinghai Lake and originated from Shulenan Mountain in Tianjun County, Qinghai Province. It has a total length of 262 km and a drainage area of 14,337 km². The elevation from the mouth to the highest mountain in the basin is 3198–5174 m.⁷⁸ The delta plain subfacies are mainly developed where the two rivers enter the lake, and the delta front and the front delta are not developed (Figures 11 and 12). The slope of the delta plain is relatively gentle, and the overall slope does not exceed 1°.

Shaliu River. The channel width of the Shaliu River is about 100 m. On the plains near the lake, there are many abandoned channels, the width of the abandoned channels is also less than 100 m, and multiple crevasse splays can be seen (Figure 11). The water source of the Shaliu River is the snow-capped water in the upper mountainous area, which is small in scale, resulting in slower flow velocity. Existing studies have shown that the annual

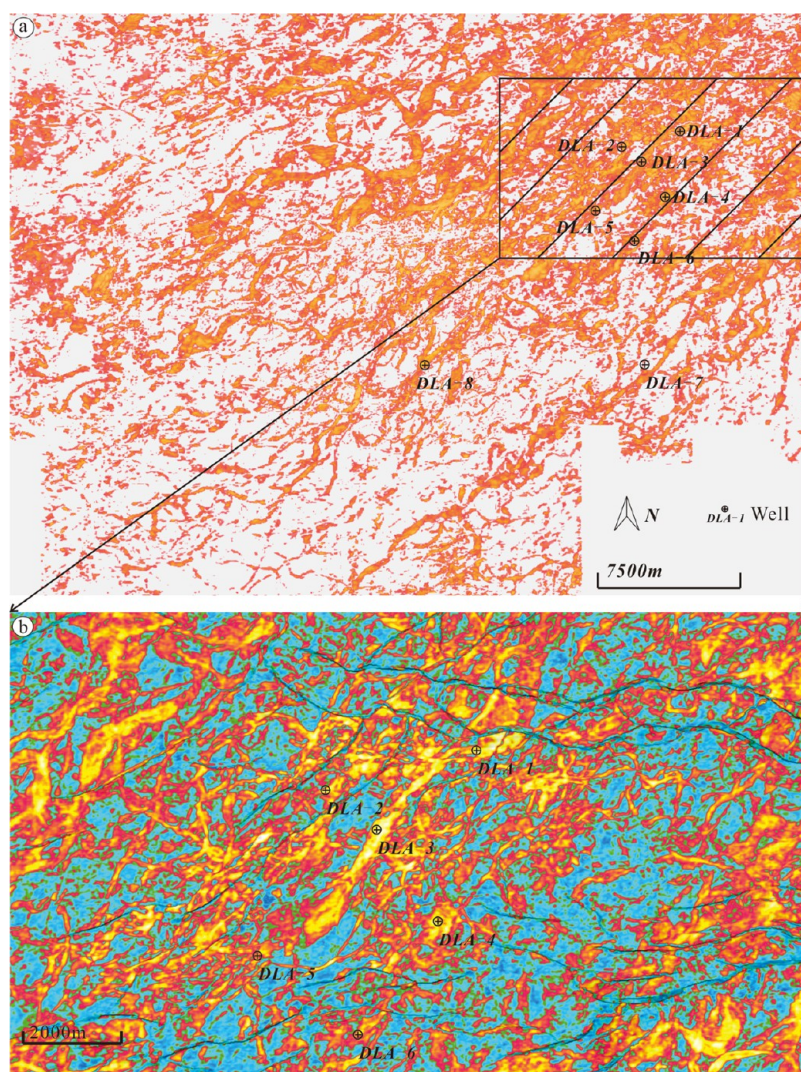


Figure 8. Channel development characteristics in the study area characterized by seismic sedimentology ((a) geobody interpretation in the study area; (b) stratigraphic slice of the box area in (a)).

average runoff of the Shaliu River is about $10 \text{ m}^3/\text{s}$,⁷⁸ indicating that the hydrodynamic conditions are obviously weak and the carrying capacity is not strong, resulting in short channels. The delta front and front delta are not developed. When a flood occurs in the upstream, the velocity and flow will increase sharply in a short period of time. The river overflows the river channel in the delta plain, forming a crevasse splay, causing pan-plainization of the downstream area near the lake, and the grain size of the sediment at the crevasse splay is smaller than that of the channels. At the same time, the advent of the flood season makes the river channel very easy to be rerouted, and the original abandoned river channel is filled under the effect of pan-plainization.

Buha River. Due to the larger area of the Buha River Basin and the longer river, there are other tributaries in addition to the snow-capped water in the basin. Existing studies have shown that the annual average runoff of Buha River is about $25 \text{ m}^3/\text{s}$.⁷⁸ Therefore, the flow rate is larger than that of the Shaliu River and the channels are wider. The channel width in the plain near the lake is about 200 m, with obvious branches, there are many abandoned channels, and the crevasse splay is very developed (Figure 12). The sedimentary characteristics after the river enters the lake are not obvious.

Through researching the literature, it is found that the water level of Qinghai Lake has changed many times in the past 50 years.⁷⁹ During the highest water level, part of the delta plain is covered by water, and the underwater channels will be transformed. The combined effects of flood overflow, river inflow, and lake dynamics also lead to pan-plainization, resulting in the deposition of thicker sand bodies mainly within the river channels. Consequently, the river channels undergo frequent changes and exhibit narrow widths. Additionally, a certain amount of sandstone deposits develop between the river channels as a result of pan-plainization. These sandstones have a thinner thickness, finer grain size, and higher mud content compared to the river channels.

The comparison with the sedimentary models of the Shaliu River in the northern part of Qinghai Lake and the Buha River in the west verifies the accuracy of the sedimentary model in the study area and further supplements the sedimentary model of the narrow channel shallow water delta. At the same time, it also reveals that sandstone reservoir deposits also exist between the river channels, which are mainly located in the blue area in Figure 10. Based on drilled well data, the thickness is mainly distributed between 1 and 3 m. The thickness of the reservoir formed by this part is thinner and the content of clay is high,

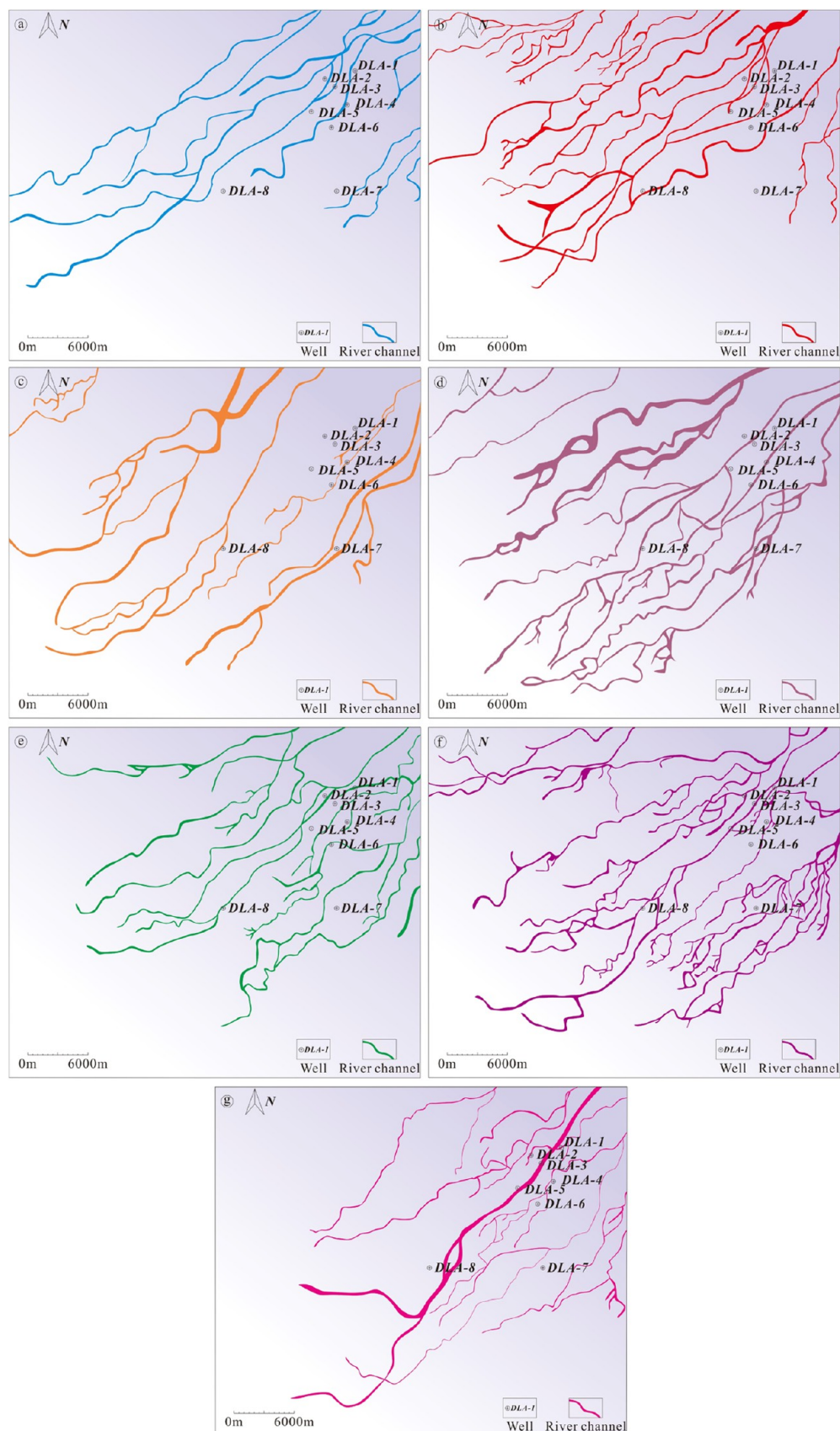


Figure 9. Channel development characteristics of the study area based on the stratal slices ((a–g) channel development characteristics of the top of the V oil group from the early to late stage).

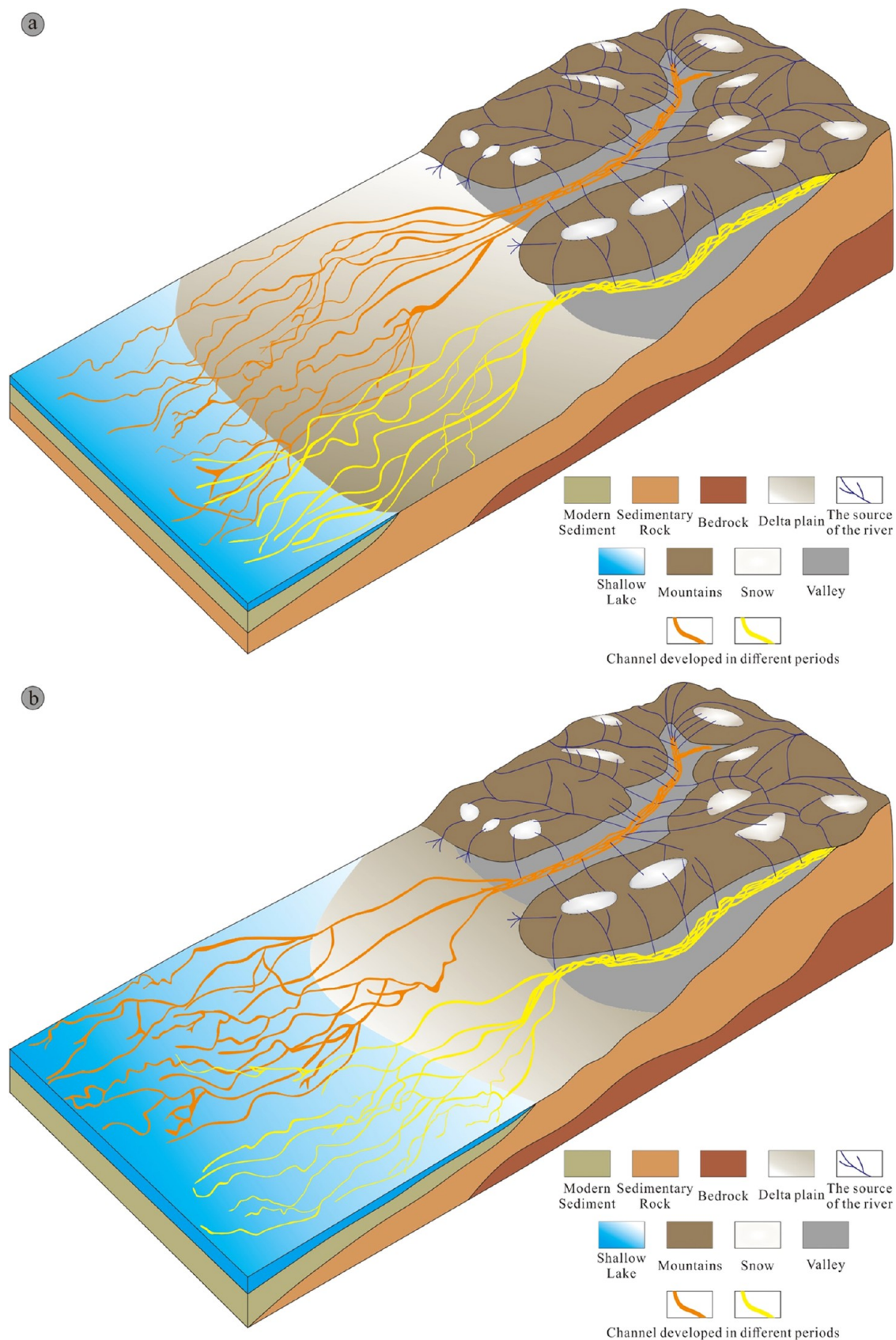


Figure 10. Sedimentary model of the extremely narrow channel shallow water delta in the study area ((a) low water level; (b) high water level).

which is difficult to identify on seismic stratal slices. And the contribution to the reserves of this part is limited. However, it has played an important role in communicating the narrow

channels system and is crucial to the oil and gas seepage in the development stage.



Figure 11. Sedimentary characteristics of Shaliu River.



Figure 12. Sedimentary characteristics of Buha River.

CONCLUSIONS

- (1) The experimental results of trace elements show that the top of the V oil group in the study area was deposited in a freshwater environment with strong oxic conditions. The changes of major and trace elements indicate that the climate in the lower part of Minghuazhen Formation was dry and cold in the early stage, and gradually changed to a warm and humid in the later stage.
- (2) The hydrodynamic conditions during the deposition of the top V oil group in the study area are generally weak and undergo frequent changes at different scales. The sedimentary discontinuities and weathering surfaces observed in the cores indicate that the study area is often exposed at the surface.
- (3) Seismic stratal slices show that during the development of the top of the V oil group in the study area, the mainstream domain gradually transitioned from northwest to southeast. In the early and late stages, narrow channels were mainly developed, while in the middle stage, the channels were wider. Moreover, in the early to late development process, the beginning of the river branch gradually moved in the direction of the source, indicating the expansion of the water body.
- (4) Comprehensive analysis shows that the formation of extremely narrow rivers in the study area is mainly related to weak hydrodynamic conditions and frequent river diversions. Weak hydrodynamic conditions lead to limited undercutting and sidecutting of rivers, and the frequent diversion of the river has hindered its stable long-term development. The combined effect of multiple factors results in the formation of extremely narrow channels.
- (5) The analysis of the sedimentary characteristics of the Shaliu River and the Buha River in Qinghai Lake confirmed the formation process of the narrow channel reservoir in the study area. The low average runoff of the river and the gentle slope of the delta plain contribute to

the slow flow of the river. Additionally, the river undergoes frequent changes, resulting in the formation of narrow channels in both the Shaliu River and Buha River.

AUTHOR INFORMATION

Corresponding Author

Xingxing Kong – CNOOC Research Institute Ltd., Beijing 100028, China; orcid.org/0000-0003-0996-1150; Email: 1214791825@qq.com

Authors

Hongjun Fan – CNOOC Research Institute Ltd., Beijing 100028, China; orcid.org/0000-0002-7623-153X

Pengfei Mu – Bohai Oilfield Research Institute, Tianjin Branch of CNOOC Ltd., Tianjin 300452, China

Dianshi Xiao – School of Geosciences, China University of Petroleum (East China), Qingdao 266580, China

Dalin Zhao – Bohai Oilfield Research Institute, Tianjin Branch of CNOOC Ltd., Tianjin 300452, China

Meijia Liu – Bohai Oilfield Research Institute, Tianjin Branch of CNOOC Ltd., Tianjin 300452, China

Mingwei He – CNOOC Research Institute Ltd., Beijing 100028, China

Complete contact information is available at:

<https://pubs.acs.org/10.1021/acsomega.3c06055>

Notes

The authors declare no competing financial interest.

ACKNOWLEDGMENTS

The authors thank the CNOOC Research Institute Ltd. and the Bohai Oilfield Research Institute for providing the opportunity to carry out this study. Further, the authors thank the DL-A oilfield project team for their support.

REFERENCES

- (1) Dai, L.; Li, J.; Zhou, X.; Cui, Z.; Cheng, J. Depositional system of the Neogene shallow water delta in Bohai Sea area. *Lithol. Reservoirs* **2007**, *19* (4), 75–81.
- (2) Wang, M.; Xie, J.; Zhang, Q.; Wang, Y.; Duan, Y. Characteristics and sedimentary model of a reticular shallow-water delta with distributary channels: lower member of the Neogene Minghuazhen Formation in the Bozhong area of the Huanghekou Sag, China. *Arabian J. Geosci.* **2019**, *12* (24), No. 760, DOI: 10.1007/s12517-019-4928-5.
- (3) Zhu, X.; Liu, Y.; Fang, Q.; Li, X.; Liu, Y.; Wang, R.; Song, J.; Liu, S.; Cao, H.; Liu, X. Formation and sedimentary model of shallow delta in large-scale lake. example from Cretaceous Quantou Formation in Sanzhao Sag, Songliao Basin. *Earth Sci. Front.* **2012**, *19* (1), 89–99.
- (4) Xin, W.; Bai, Y.; Xu, H. Experimental study on evolution of lacustrine shallow-water delta. *Catena* **2019**, *182*, No. 104125.
- (5) Zeng, H.; Zhao, X.; Zhu, X.; Jin, F.; Dong, Y.; Wang, Y.; Zhu, M.; Zheng, R. Seismic sedimentology of sub-clinoformal shallow-water meandering river delta: A case from the Suning area of Raoyang sag in Jizhong depression, Bohai Bay Basin, NE China. *Pet. Explor. Dev.* **2015**, *42* (5), 621–632.
- (6) Yingchang, C.; Min, H.; Yanzhong, W.; Mingyou, T.; Yingge, Z. Sedimentary characteristics and models of shallow-water delta deposits in the second member of the Shahejie Formation in the Chezhen Sag, the Jiyang Depression. *Oil Gas Geol.* **2010**, *31* (5), 576–582, DOI: 10.19389/j.cnki.1003-0506.2023.02.019.
- (7) Zhang, L.; Bao, Z.; Lin, Y.; Chen, Y.; Liu, X.; Dou, L.; Kong, B. Genetic types and sedimentary model of sandbodies in a shallow-water delta: A case study of the first Member of Cretaceous Yaojia Formation in Qian'an area, south of Songliao Basin, NE China. *Pet. Explor. Dev.* **2017**, *44* (5), 770–779, DOI: 10.1016/S1876-3804(17)30087-3.
- (8) Lou, Z.; Lan, X.; Lu, Q.; Cai, X. Controls of the topography, climate and lake level fluctuation on the depositional environment of a shallow-water delta: A case study of the Cretaceous Putaohua reservoir in the northern part of Songliao Basin. *Acta Geol. Sin.* **1999**, *73* (1), 83–92.
- (9) Zhu, X.; Li, S.; Wu, D.; Zhu, S.; Dong, Y.; Zhao, D.; Wang, X.; Zhang, Q. Sedimentary characteristics of shallow-water braided delta of the Jurassic, Junggar basin, Western China. *J. Pet. Sci. Eng.* **2017**, *149*, 591–602.
- (10) Zhu, X.; Zeng, H.; Li, S.; Dong, Y.; Zhu, S.; Zhao, D.; Huang, W. Sedimentary characteristics and seismic geomorphologic responses of a shallow-water delta in the Qingshankou Formation from the Songliao Basin, China. *Mar. Pet. Geol.* **2017**, *79*, 131–148.
- (11) Zhang, C.; Yin, T.; Zhu, Y.; Ke, L.-m. Shallow-water deltas and models. *Acta Sedimentol. Sin.* **2010**, *28* (5), 933–944.
- (12) Gilbert, G. K. *The Topographic Features of Lake Shores*; US Government Printing Office, 1885.
- (13) Lemons, D. R.; Chan, M. A. Facies architecture and sequence stratigraphy of fine-grained lacustrine deltas along the eastern margin of late Pleistocene Lake Bonneville, northern Utah and southern Idaho. *AAPG Bull.* **1999**, *83* (4), 635–665, DOI: 10.1306/00AA9C14-1730-11D7-8645000102C1865D.
- (14) Fisk, H. N.; Kolb, C. R.; McFarlan, E.; Wilbert, L. J. Sedimentary framework of the modern Mississippi delta [Louisiana]. *J. Sediment. Res.* **1954**, *24* (2), 76–99.
- (15) Donaldson, A. C. Pennsylvanian sedimentation of central Appalachians. In *Geological Society of America*; GeoScienceWorld, 1974 DOI: 10.1130/SPE148-p47.
- (16) Donaldson, A. C.; Briggs, G. Pennsylvanian Sedimentation of Central Appalachians. In *Carboniferous of the Southeastern United States*; Geological Society of America, 1974; Vol. 148, p 0.
- (17) Lou, Z.; Lu, Q.; Cai, X. Influence of lake level fluctuation on sandbody shapes at shallow-water delta front. *Acta Sedimentol. Sin.* **1998**, *16* (4), 27–31.
- (18) Xuanjun, Y.; Hongying, Z.; Zhijie, Z.; Ziye, W.; Dawei, C.; Hao, G. U. O.; Youyan, Z.; Wentong, D. Depositional features and growth pattern of large shallow-water deltas in depression basin. *Lithol. Reservoirs* **2021**, *33* (1), 1–11.
- (19) Huang, X.; Liu, K.; Zou, C.; Yuan, X.; Gui, L. Forward stratigraphic modelling of the shallow-water delta system in the Poyang Lake, southern China. *J. Geochem. Explor.* **2014**, *144*, 74–83, DOI: 10.1016/j.gexplo.2014.01.019.
- (20) Zhu, X.; Zhang, Y.; Yang, J.; Li, D.; Zhang, N. Sedimentary characteristics of the shallow Jurassic braided river delta, the Junggar Basin. *Oil Gas Geol.* **2008**, *29*, 244–251.
- (21) Zhu, W.; Li, J.; Zhou, X.; Guo, Y. Neogene shallow water deltaic system and large hydrocarbon accumulations in Bohai Bay, China. *Acta Sedimentol. Sin.* **2008**, *26* (4), 575–582.
- (22) Zou, C.; Zhao, W.; Zhang, X.; Luo, P.; Wang, L.; Liu, L.; Xue, S.; Yuan, X.; Zhu, R.; Tao, S. Formation and distribution of shallow-water deltas and central-basin sandbodies in large open depression lake basins. *Acta Geol. Sin.* **2008**, *82* (6), 813–825.
- (23) Li, J.; Liu, H.; Niu, C.; Guo, R.; Wang, Y. Evolution regularity of the Neogene shallow water delta in the Laibei area Bohai Bay Basin, northern China. *J. Palaeogeogr.* **2014**, *3* (3), 257–269, DOI: 10.3724/SP.J.1261.2014.00055.
- (24) Yang, Y.; Xu, T. Hydrocarbon habitat of the offshore Bohai Basin, China. *Mar. Pet. Geol.* **2004**, *21* (6), 691–708.
- (25) Xu, S.; Hao, F.; Xu, C.; Zou, H.; Zhang, X.; Zong, Y.; Zhang, Y.; Cong, F. Hydrocarbon migration and accumulation in the northwestern Bozhong subbasin, Bohai Bay Basin, China. *J. Pet. Sci. Eng.* **2019**, *172*, 477–488.
- (26) Xu, C.; Yang, H.; Wang, D.; Zhao, D.; Wang, L. Formation conditions of Neogene large-scale high-abundance lithologic reservoir in the Laibei low uplift, Bohai Sea, East China. *Pet. Explor. Dev.* **2021**, *48* (1), 15–29.

- (27) Xu, S.; Hao, F.; Xu, C.; Zou, H.; Gao, B. Seismic geomorphology and sedimentology of a fluvial-dominated delta: Implications for the Neogene reservoirs, offshore Bohai Bay Basin, China. *AAPG Bull.* **2019**, *103* (10), 2399–2420.
- (28) Xu, C.; Jiang, P.; Wu, F.; Yang, B.; Li, D. Discovery and sedimentary characteristics of the Neogene delta in Bozhong depression and its significance for oil and gas exploration. *Acta Sedimentol. Sin.* **2002**, *20* (4), 588–594.
- (29) Xu, S.; Hao, F.; Xu, C.; Zou, H.; Zhang, X.; Zhang, Y.; Gao, B.; Wang, Q. Gravity-flow deposits and their exploration prospects in the Oligocene Dongying Formation, northwestern Bozhong Subbasin, Bohai Bay Basin, China. *Mar. Pet. Geol.* **2018**, *96*, 179–189.
- (30) Hao, S.; Liu, H.; Du, X.; Niu, C. Sedimentary characteristics of shallow-water delta and responses features in palaeoenvironment: a case study from the lower part of Neogene Minghuazhen Formation (Bonan area, Bohai Bay Basin, E China). *Arabian J. Geosci.* **2021**, *14* (4), 1–20, DOI: 10.1007/s12517-021-06572-y.
- (31) Tian, L.; Liu, H.; Niu, C.; Du, X.; Yang, B.; Lan, X.; Chen, D. Development characteristics and controlling factor analysis of the Neogene Minghuazhen Formation shallow water delta in Huanghekou area, Bohai offshore basin. *J. Palaeogeogr.* **2019**, *8* (1), 19 DOI: 10.1186/s42501-019-0032-8.
- (32) Zhou, X.; Lü, X.; Liu, C. Geochemical characteristics of carbonates and indicative significance of the sedimentary environment based on carbon-oxygen isotopes, trace elements and rare earth elements: case study of the Lower Paleozoic carbonates in the Gucheng area, Tarim Basin, China. *Arabian J. Geosci.* **2021**, *14* (14), 1–18, DOI: 10.1007/s12517-021-07574-6.
- (33) Wang, M.; Guo, Z.; Jiao, C.; Lu, S.; Li, J.; Xue, H.; Li, J.; Li, J.; Chen, G. Exploration progress and geochemical features of lacustrine shale oils in China. *J. Pet. Sci. Eng.* **2019**, *178*, 975–986.
- (34) Li, W.; Zhang, Z.; Zheng, K.; Li, Y. geochemical characteristics and developmental models of the Eocene source rocks in the Qiongdongnan basin, northern south China sea. *Energy Fuels* **2017**, *31* (12), 13487–13493.
- (35) He, T.; Li, W.; Lu, S.; Pan, W.; Ying, J.; Zhu, P.; Yang, E.; Wang, X.; Zhang, B.; Sun, D. Mechanism and geological significance of anomalous negative $\delta^{13}\text{C}$ kerogen in the Lower Cambrian, NW Tarim Basin, China. *J. Pet. Sci. Eng.* **2022**, *208*, No. 109384.
- (36) He, T.; Lu, S.; Li, W.; Wang, W.; Sun, D.; Pan, W.; Zhang, B. Geochemical characteristics and effectiveness of thick, black shales in southwestern depression, Tarim Basin. *J. Pet. Sci. Eng.* **2020**, *185*, No. 106607.
- (37) Zhang, L.; Xiao, D.; Lu, S.; Jiang, S.; Lu, S. Effect of sedimentary environment on the formation of organic-rich marine shale: Insights from major/trace elements and shale composition. *Int. J. Coal Geol.* **2019**, *204*, 34–50.
- (38) He, T.; Lu, S.; Li, W.; Sun, D.; Pan, W.; Zhang, B.; Tan, Z.; Ying, J. Paleoweathering, hydrothermal activity and organic matter enrichment during the formation of earliest Cambrian black strata in the northwest Tarim Basin, China. *J. Pet. Sci. Eng.* **2020**, *189*, No. 106987.
- (39) Wei, W.; Algeo, T. J. Elemental proxies for paleosalinity analysis of ancient shales and mudrocks. *Geochim. Cosmochim. Acta* **2020**, *287*, 341–366.
- (40) Chen, Z.; Chen, Z.; Zhang, W. Quaternary stratigraphy and trace-element indices of the Yangtze Delta, Eastern China, with special reference to marine transgressions. *Quat. Res.* **1997**, *47* (2), 181–191.
- (41) Wang, Y.; Guo, W.; Zhang, G. Application of some geochemical indicators in determining of sedimentary environment of the Funing Group (Paleogene), Jin-Hu Depression, Kiangsu Province. *J. Tongji Univ.* **1979**, *7* (2), 51–60.
- (42) Zuo, X.; Li, C.; Zhang, J.; Ma, G.; Chen, P. Geochemical characteristics and depositional environment of the Shahejie Formation in the Binnan Oilfield, China. *J. Geophys. Eng.* **2020**, *17* (3), 539–551.
- (43) Li, W.; Zhang, Z.; Li, Y.; Fu, N. The effect of river-delta system on the formation of the source rocks in the Baiyun Sag, Pearl River Mouth Basin. *Mar. Pet. Geol.* **2016**, *76*, 279–289.
- (44) Li, W.; Zhang, Z. Paleoenvironment and its control of the formation of Oligocene marine source rocks in the deep-water area of the northern South China Sea. *Energy Fuels* **2017**, *31* (10), 10598–10611.
- (45) Tribouillard, N.; Algeo, T. J.; Lyons, T.; Riboulleau, A. Trace metals as paleoredox and paleoproductivity proxies: An update. *Chem. Geol.* **2006**, *232* (1–2), 12–32.
- (46) Jones, B.; Manning, D. A. Comparison of geochemical indices used for the interpretation of palaeoredox conditions in ancient mudstones. *Chem. Geol.* **1994**, *111* (1–4), 111–129.
- (47) Cao, H.; Guo, W.; Shan, X.; Ma, L.; Sun, P. Paleolimnological environments and organic accumulation of the Nenjiang formation in the southeastern Songliao Basin, China. *Oil Shale* **2015**, *32*, No. 1, DOI: 10.3176/oil.2015.1.02.
- (48) Lin, Z.; Chen, D.; Liu, Q. Geochemical indices for redox conditions of marine sediments. *Bull. Mineral., Petrol. Geochem.* **2008**, *27* (1), 72–80.
- (49) Algeo, T. J.; Li, C. Redox classification and calibration of redox thresholds in sedimentary systems. *Geochim. Cosmochim. Acta* **2020**, *287*, 8–26.
- (50) Liang, W.; Xiao, C.; Xiao, S. Study on Relationships between Paleoenvironment, Paleoclimate of Middle Permian-middle Triassic and Constant, Trace Elements in Western Sichuan. *Technol. Eng.* **2015**.
- (51) Gebregiorgis, D.; Deocampo, D. M.; Foerster, V.; Longstaffe, F. J.; Delaney, J. S.; Schaebitz, F.; Junginger, A.; Markowska, M.; Opitz, S.; Trauth, M. H. Modern sedimentation and authigenic mineral formation in the Chew Bahir Basin, southern Ethiopia: implications for interpretation of Late Quaternary paleoclimate records. *Front. Earth Sci.* **2021**, *9*, No. 607695, DOI: 10.3389/feart.2021.607695.
- (52) Song, H.; Guo, X.; He, L. Geochemical characteristics of paleosols from Late Devonian and its paleoclimatic significance. *Chin. J. Geol.* **2019**, *54* (4), 1252–1264, DOI: 10.12017/dzcx.2019.071.
- (53) Liu, J.; Ma, X.; Lin, C.; Ynag, H.; Shu, Z.; Fu, C.; Lothar, S. *The Silurian Red Beds of Tarim Basin: Signals of Paleoenvironment, Paleoclimate and Sea Level Change*, 80th EAGE Conference and Exhibition 2018, Vol. 208; European Association of Geoscientists & Engineers, 2018; pp 1–5.
- (54) Adams, J. S.; Kraus, M. J.; Wing, S. L. Evaluating the use of weathering indices for determining mean annual precipitation in the ancient stratigraphic record. *Palaeogeogr., Palaeoclimatol., Palaeoecol.* **2011**, *309* (3–4), 358–366.
- (55) Fu, J.; Li, S.; Xu, L.; Niu, X. Paleo-sedimentary environmental restoration and its significance of Chang 7 Member of Triassic Yanchang Formation in Ordos Basin, NW China. *Pet. Explor. Dev.* **2018**, *45* (6), 998–1008.
- (56) Nesbitt, H.; Young, G. Ancient Climatic and Tectonic Settings Inferred from Paleosols Developed on Igneous Rocks. In *The Precambrian Earth: Tempos and Events*; Elsevier: Amsterdam, 2004; pp 482–493.
- (57) Fedo, C. M.; Wayne Nesbitt, H.; Young, G. M. Unraveling the effects of potassium metasomatism in sedimentary rocks and paleosols, with implications for paleoweathering conditions and provenance. *Geology* **1995**, *23* (10), 921–924.
- (58) Nesbitt, H.; Young, G. M. Early Proterozoic climates and plate motions inferred from major element chemistry of lutites. *nature* **1982**, *299* (5885), 715–717.
- (59) Nesbitt, H. W.; Young, G. M. Prediction of some weathering trends of plutonic and volcanic rocks based on thermodynamic and kinetic considerations. *Geochim. Cosmochim. Acta* **1984**, *48* (7), 1523–1534.
- (60) Suttner, L. J.; Dutta, P. K. Alluvial sandstone composition and paleoclimate; I, Framework mineralogy. *J. Sediment. Res.* **1986**, *56* (3), 329–345, DOI: 10.1306/212F8909-2B24-11D7-8648000102C1865D.
- (61) Ghosh, S.; Sarkar, S. Geochemistry of Permo-Triassic mudstone of the Satpura Gondwana basin, central India: clues for provenance. *Chem. Geol.* **2010**, *277* (1–2), 78–100.
- (62) Hofmann, M.; Li, X.; Chen, J.; MacKenzie, L.; Hinman, N. Provenance and temporal constraints of the early Cambrian

Maotianshan shale, Yunnan Province, China. *Gondwana Res.* **2016**, *37*, 348–361.

(63) Fathy, D.; Wagreich, M.; Gier, S.; Mohamed, R. S.; Zaki, R.; El Nady, M. M. Maastrichtian oil shale deposition on the southern Tethys margin, Egypt: Insights into greenhouse climate and paleoceanography. *Palaeogeogr., Palaeoclimatol., Palaeoecol.* **2018**, *505*, 18–32.

(64) Wang, Y.; Li, G.; Zhang, W.; Dong, P. Sedimentary environment and formation mechanism of the mud deposit in the central South Yellow Sea during the past 40 kyr. *Mar. Geol.* **2014**, *347*, 123–135.

(65) Lee, K.; Gihm, Y. S. Downstream changes in floodplain sedimentation and their effects on channel avulsion in stream-dominated alluvial fans: The cretaceous Duwon Formation in the southern Korean Peninsula. *Sediment. Geol.* **2023**, *456*, No. 106473, DOI: [10.1016/j.sedgeo.2023.106473](https://doi.org/10.1016/j.sedgeo.2023.106473).

(66) Tao, L.; Sun, P.; Xu, Y. Sedimentary origin of fine-grained rocks in the Permian Lucaogou Formation in the southern Junggar Basin: implications from grain size analysis. *Geomech. Geophys. Geoenergy Geosour.* **2022**, *8* (6), No. 192, DOI: [10.1007/s40948-022-00475-2](https://doi.org/10.1007/s40948-022-00475-2).

(67) Chu, G.; Sun, Q.; Yang, K.; Li, A.; Yu, X.; Xu, T.; Yan, F.; Wang, H.; Liu, M.; Wang, X. Evidence for decreasing South Asian summer monsoon in the past 160 years from varved sediment in Lake Xinluhai, Tibetan Plateau. *J. Geophys. Res.: Atmos.* **2011**, *116* (D2), No. 014454, DOI: [10.1029/2010JD014454](https://doi.org/10.1029/2010JD014454).

(68) Liu, X.; Yu, Z.; Dong, H.; Chen, H.-F. A less or more dusty future in the Northern Qinghai-Tibetan Plateau? *Sci. Rep.* **2014**, *4* (1), No. 6672, DOI: [10.1038/srep06672](https://doi.org/10.1038/srep06672).

(69) Zhao, K.; Du, X.; Lu, Y.; Xiong, S.; Wang, Y. Are light-dark coupled laminae in lacustrine shale seasonally controlled? A case study using astronomical tuning from 42.2 to 45.4 Ma in the Dongying Depression, Bohai Bay Basin, eastern China. *Palaeogeogr., Palaeoclimatol., Palaeoecol.* **2019**, *528*, 35–49.

(70) Zeng, H.; Zhu, X.; Zhu, R.; Zhang, Q. Guidelines for seismic sedimentologic study in non-marine postrift basins. *Pet. Explor. Dev.* **2012**, *39* (3), 295–304.

(71) Yin, X.; Lu, S.; Wang, P.; Wang, Q.; Wang, W.; Yao, T. A three-dimensional high-resolution reservoir model of the Eocene Shahejie Formation in Bohai Bay Basin, integrating stratigraphic forward modeling and geostatistics. *Mar. Pet. Geol.* **2017**, *82*, 362–370.

(72) Yin, X.; Huang, W.; Lu, S.; Wang, P.; Wang, W.; Xia, L.; Yao, T. The connectivity of reservoir sand bodies in the Liaoxi sag, Bohai Bay basin: Insights from three-dimensional stratigraphic forward modeling. *Mar. Pet. Geol.* **2016**, *77*, 1081–1094.

(73) Zeng, H.; Backus, M. M.; Barrow, K. T.; Tyler, N. Stratal slicing, part I: realistic 3-D seismic model. *Geophysics* **1998**, *63* (2), 502–513.

(74) Zeng, H.; Henry, S. C.; Riola, J. P. Stratal slicing, Part II: Real 3-D seismic data. *Geophysics* **1998**, *63* (2), 514–522.

(75) Zeng, H.; Backus, M. M. Interpretive advantages of 90°-phase wavelets: Part 2—Seismic applications. *Geophysics* **2005**, *70* (3), C17–C24.

(76) Xu, S.; Hao, F.; Xu, C.; Wang, Y.; Zou, H.; Gong, C. Differential compaction faults and their implications for fluid expulsion in the northern Bozhong Subbasin, Bohai Bay Basin, China. *Mar. Pet. Geol.* **2015**, *63*, 1–16.

(77) Xu, S.; Hao, F.; Xu, C.; Zou, H.; Tian, J. Tracing migration pathways by integrated geological, geophysical, and geochemical data: A case study from the JX1–1 oil field, Bohai Bay Basin, China. *AAPG Bull.* **2014**, *98* (10), 2109–2129.

(78) Li, Y.; Li, X.; Cui, B.; Peng, H.; Yi, W. Trend of streamflow in Lake Qinghai basin during the past 50 years (1956–2007)—Take Buha River and Shaliu River for examples. *J. Lake Sci.* **2010**, *22* (5), 757–766.

(79) Luo, C.; Xu, C.; Cao, Y.; Tong, L. Monitoring of water surface area in Lake Qinghai from 1974 to 2016. *J. Lake Sci.* **2017**, *29* (5), 1245–1253, DOI: [10.18307/2017.0523](https://doi.org/10.18307/2017.0523).